Catalysis Today 138 (2008) 152–156

Contents lists available at ScienceDirect

Catalysis Today

journal homepage: www.elsevier.com/locate/cattod

Autothermal reforming of ethanol for hydrogen production over an Rh/CeO_2 catalyst

Weijie Cai [a,b], Fagen Wang [a], A.C. Van Veen [b], H. Provendier [b], C. Mirodatos [b], Wenjie Shen [a,*]

[a] State Key Laboratory of Catalysis, Dalian Institute of Chemical Physics, Chinese Academy of Sciences, 457 Zhongshan Road, Dalian 116023, China
[b] University of Lyon - Institut de Recherches sur la Catalyse et l'Environnement de Lyon (IRCELYON, UMR 5256, CNRS - Université Claude Bernard Lyon1), 69626 Villeurbanne Cedex, France

ARTICLE INFO

Article history:
Available online 7 July 2008

Keywords:
Ethanol
Hydrogen
Autothermal reforming
Rh/CeO_2

ABSTRACT

Hydrogen production from ethanol by autothermal reforming over an Rh/CeO_2 catalyst was investigated with a stoichiometric feed composition. Ethanol as well as the reaction intermediates like acetaldehyde and acetone was entirely converted to hydrogen and C1 products at 673 K, and methane steam reforming and reverse water gas shift were the major reactions above 823 K. The Rh/CeO_2 catalyst exhibited stable activity and selectivity during 70 h on-stream operation at 823–923 K without obvious deactivation evidenced by the constant effluent gas composition. Structural analysis of the used catalyst revealed that CeO_2 prevented effectively the highly dispersed Rh particles with sizes of 1–3 nm from sintering and thus maintained sufficient Rh–CeO_2 interfacial areas, which facilitated coke gasification through the high oxygen storage-release capacity.

© 2008 Elsevier B.V. All rights reserved.

1. Introduction

Hydrogen production from ethanol has attracted a growing interest in fueling proton exchanged membrane fuel cells. Steam reforming and autothermal reforming are identified to be effective routes for producing hydrogen from ethanol [1]. In the last years, steam reforming of ethanol has received more attention due to its relatively higher hydrogen productivity [1–5]. Liguras et al. [6] found that among the low-loaded catalysts, Rh was significantly more active and selective towards hydrogen formation than Ru, Pt and Pd. Kinetic measurements also revealed that Rh was 2.3, 3.7 and 5.8 times more active than Pd, Co and Ni, respectively [7]. The excellent activity of Rh catalyst is mainly due to the capacity of Rh to break the carbon–carbon bond necessary for an efficient total decomposition of ethanol [8]. However, steam reforming of ethanol is an endothermic process which requires energy input to initiate the reaction.

Autothermal reforming, also called oxidative steam reforming, is a combination of ethanol oxidation and steam reforming, providing a reasonable compromise between energy efficiency and hydrogen yield. Using ethanol, water and oxygen mixture with a molar ratio of 1:1.8:0.6, the overall reaction can be thermally neutral in which the exothermic oxidation of ethanol provides the heat necessary for the concurrent endothermic steam reforming of ethanol [9]. Moreover, the presence of oxygen in the reaction mixture also promotes the efficient removal of carbon species formed during the course of reaction. Deluga et al. [10] developed a millisecond-contact time reactor for efficient autothermal reforming of ethanol using an Rh/CeO_2 catalyst with very high activity and selectivity. Kugai et al. [11] found that the addition of Ni to Rh/CeO_2 catalysts greatly improved the dispersion of Rh particles, leading to higher catalytic activity.

In this work, we investigated autothermal reforming of ethanol over an Rh/CeO_2 catalyst with the focus on hydrogen productivity and reaction stability. The results indicated that the Rh/CeO_2 catalyst had a rather high level of stability for autothermal reforming of ethanol even with stoichiometric feed composition at 823–923 K.

2. Experimental

2.1. Catalyst preparation

The CeO_2 support was prepared by precipitating ammonia cerium nitrate with urea, as described elsewhere [9]. The Rh/CeO_2 catalyst with an Rh loading of 1 wt.% was prepared by the deposition–precipitation method. CeO_2 powder was suspended in aqueous solution containing certain amounts of Rh precursor ($RhCl_3 \cdot nH_2O$) and the mixture was heated to 348 K with stirring. A 0.1 M Na_2CO_3 aqueous solution was added gradually until the pH

---

[*] Corresponding author. Tel.: +86 411 84379085; fax: +86 411 84694447.
E-mail address: shen98@dicp.ac.cn (W. Shen).

0920-5861/$ – see front matter © 2008 Elsevier B.V. All rights reserved.
doi:10.1016/j.cattod.2008.05.019

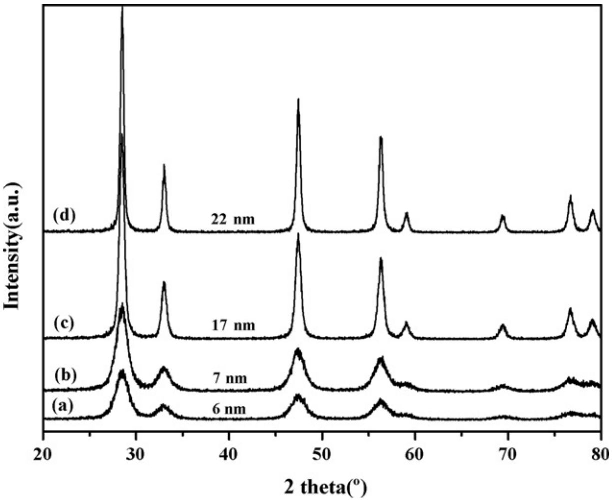

Fig. 1. XRD patterns of the CeO_2 support (a), the as-prepared Rh/CeO_2 catalyst (b) and the Rh/CeO_2 catalysts used at 823 K (c) and 923 K (d) for 70 h on-stream operations.

value of the mixture reached 9.0, followed by aging for 1 h. After filtration and washing with water, the precipitate was dried at 373 K overnight and calcined at 673 K for 5 h in air.

2.2. Catalyst characterization

N_2 adsorption–desorption isotherms were recorded at 77 K using a Nova 4200e (Quantachrome) instrument. Before the measurements, the sample was degassed at 573 K for 2 h.

X-ray power diffraction (XRD) patterns were recorded using a Rigaku D/MAX-RB diffractor with Cu Kα radiation source operated at 40 kV and 100 mA. The mean crystallite sizes of CeO_2 were calculated from the Scherrer equation [12].

HRTEM images were taken on a Philips Tecnai $G^2$20 microscope operated at 200 kV. Specimens were prepared by ultrasonically suspending the sample in ethanol. A drop of the suspension was deposited on a thin carbon film supported on a standard copper grid and dried in air.

Hydrogen temperature programmed reduction (H_2-TPR) was carried out with a conventional setup equipped with a TCD. 100 mg (40–60 mesh) samples were pretreated at 573 K for 1 h under N_2 flow (40 ml/min). After cooling to room temperature and introducing the reduction agent of a 5 vol%H_2/N_2 mixture (40 ml/min), the temperature was then programmed to rise at 10 K/min.

Oxygen storage capacity (OSC) was measured in a micro-reactor coupled to a quadrupole mass spectrometer (Omnistar, Balzers). Before analysis, the samples (100 mg) were reduced with a 5 vol%H_2/Ar mixture (50 ml/min) at 1173 K. After cooling to 723 K under Ar flow, a 5 vol%O_2/Ar mixture (50 ml/min) was passed through the sample. Oxygen consumption was calculated from the curve corresponding to $m/e = 32$ detected by the mass spectrometer.

2.3. Catalytic measurements

Autothermal reforming of ethanol was conducted with a continuous-flow fixed-bed quartz tubular reactor at atmospheric pressure. 300 mg of catalyst (40–60 mesh) were loaded and sandwiched by two layers of quartz wool. Before the reaction, the catalyst was reduced with a 5 vol%H_2/He mixture (30 ml/min) at 673 K for 3 h. A premixed ethanol/water solution with a H_2O/C_2H_5OH molar ratio of 1.8:1 was fed by a micropump to a vaporizer heated to 473 K and the vapors were then mixed with an oxygen stream coming from a mass-flow controller, giving a stoichiometric feed stream with ethanol/water/O_2 molar ratio of 1:1.8:0.6. The effluent was analyzed by on-line gas chromatography equipped with TCD and FID. The concentrations of the outlet products were calculated by excluding water, that is, dry-based gas composition.

3. Results and discussion

3.1. Physical and chemical characteristics of the Rh/CeO_2 catalyst

The specific surface areas of the CeO_2 support and the Rh/CeO_2 catalyst were 158 and 146 m^2/g, respectively, suggesting that the loading of Rh decreased the surface area of the ceria support only slightly. Fig. 1 shows the XRD patterns of the CeO_2 support and the Rh/CeO_2 catalyst: only diffraction peaks of ceria with fluorite structure were observed in the as-prepared Rh/CeO_2 catalyst and the average crystalline size was ~7 nm. There were no diffraction peaks assigned to Rh species, indicating that Rh particles were highly dispersed on CeO_2 and were too small to be detected. Fig. 2 shows the HRTEM images of the Rh/CeO_2 catalyst. CeO_2 crystallites with well-defined edges were clearly observed and the particle diameters of CeO_2 were around 5–10 nm. However, the Rh particles were hardly observed, probably due to their small sizes.

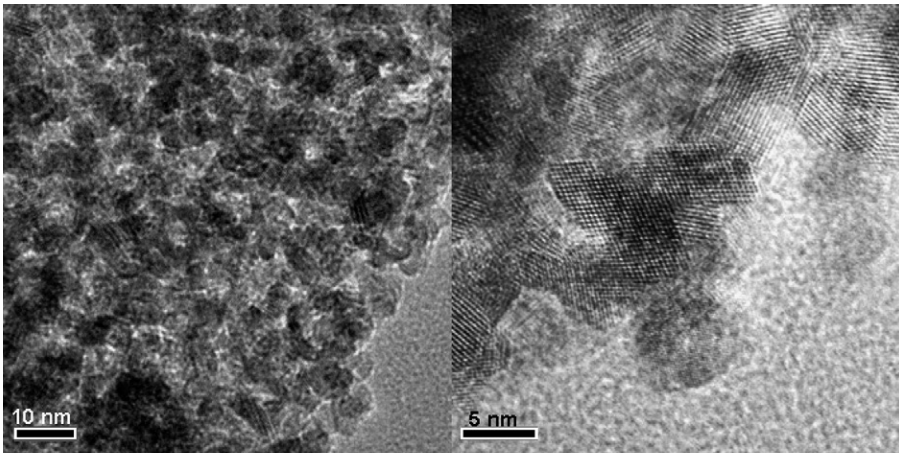

Fig. 2. HRTEM images of the as-prepared Rh/CeO_2 catalyst.

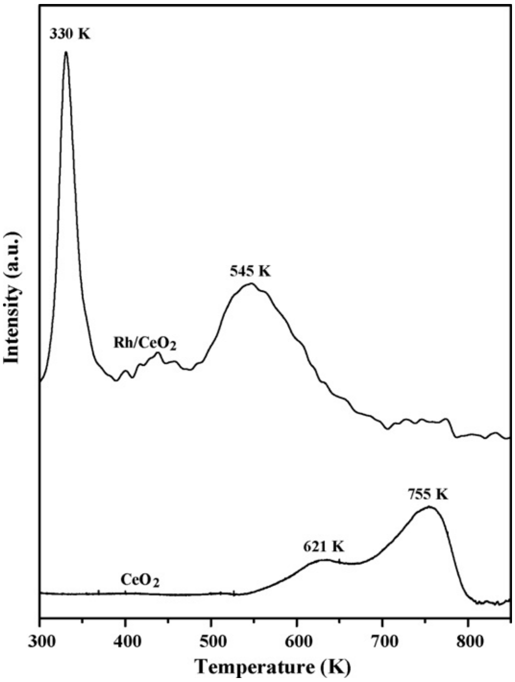

Fig. 3. H_2-TPR profiles of the CeO_2 support and the Rh/CeO_2 catalyst.

Fig. 3 compares the H_2-TPR profiles of the CeO_2 support and the Rh/CeO_2 catalyst. For CeO_2 alone, there was a broad reduction peak at ~755 K with a small shoulder at 621 K, representing the reduction of surface CeO_2 [9,13]. In the case of the Rh/CeO_2 catalyst, two main reduction peaks at 330 and 545 K were observed. The amount of hydrogen consumed at 330 K was 575 μmol/g, which was much larger than the amount needed for the reduction of Rh_2O_3 to Rh. It seemed that this hydrogen consumption was a combined reduction of Rh_2O_3 to Rh and surface reduction of CeO_2 to $CeO_{1.92}$. Accordingly, the reduction peak at 545 K with hydrogen consumption of 789 μmol/g was attributed to the further reduction of $CeO_{1.92}$ to $CeO_{1.78}$. It is clear that the reduction of CeO_2 has been greatly promoted with the addition of Rh, and the strong Rh–CeO_2 interaction shifted the reduction temperature of ceria to much lower temperatures [13].

The strong Rh–CeO_2 interaction is further evidenced by the oxygen storage capacities. The OSC of the Rh/CeO_2 catalyst (857 μmol/g) was significantly greater than that of the ceria support (421 μmol/g), demonstrating the promotion effect of Rh through which the rhodium oxide clusters diffused into the ceria fluorite structure, acting as privileged pathway for oxygen diffusion and storage [13–15].

3.2. Influence of reaction temperature

Fig. 4 shows the temperature dependence of ethanol autothermal reforming over the Rh/CeO_2 catalyst. Ethanol as well as the reaction intermediates, like acetaldehyde and acetone, was entirely converted to hydrogen and C1 products at 673 K, indicating the high activity of the Rh/CeO_2 catalyst. Idriss and co-workers [16,17] proposed that Rh favored the dissociation of C–C bond due to the lower intrinsic activation barrier. The concentration of hydrogen increased progressively with temperature, whereas the concentrations of CO_2 and CH_4 decreased gradually. At the temperatures below 823 K, the lower concentration of CO is due to the water gas shift (WGS) reaction which converted CO, once formed, into CO_2. At the temperatures above 823 K, the concentration of CO increased rapidly and the

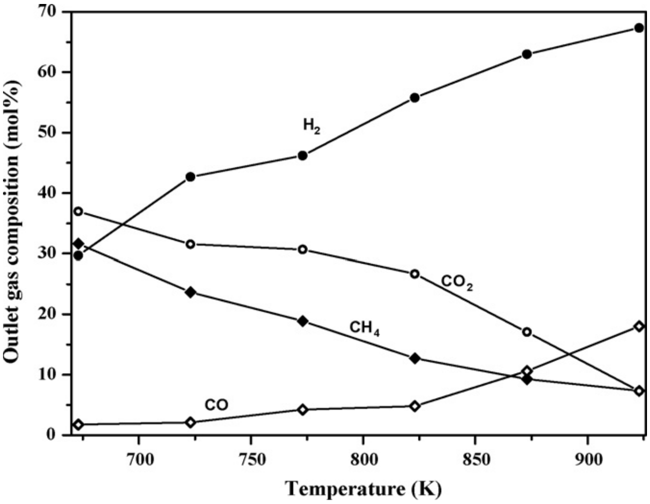

Fig. 4. Effect of reaction temperature on the product distribution of ethanol autothermal reforming over the Rh/CeO_2 catalyst. $C_2H_5OH/H_2O/O_2$ = 1:1.8:0.6 (molar ratio); contact time = 0.6 s g/ml.

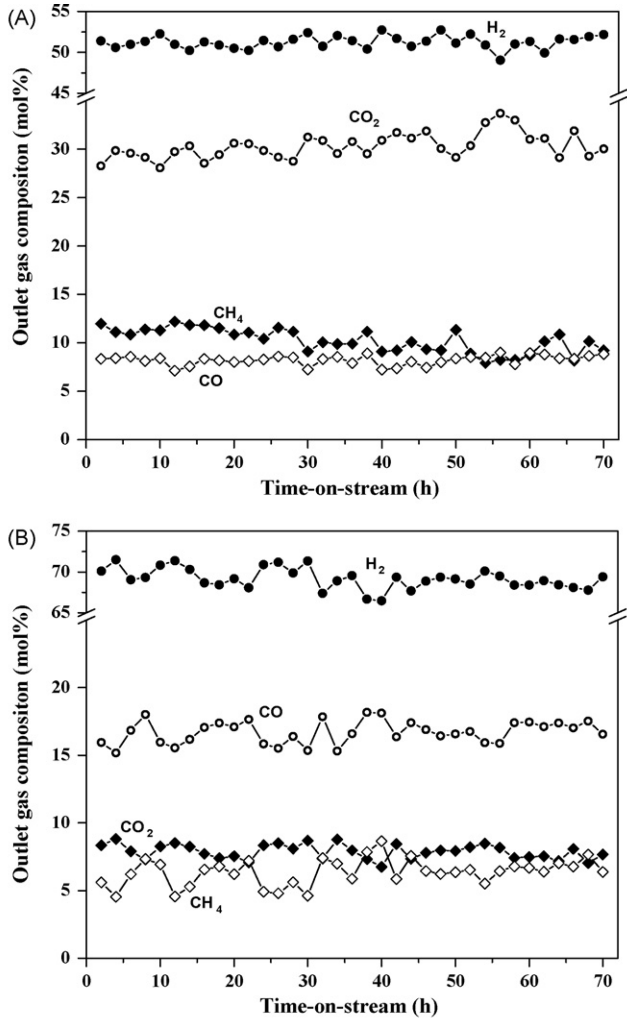

Fig. 5. Changes in the outlet gas composition during autothermal reforming of ethanol over the Rh/CeO_2 catalyst at 823 K (A) and 923 K (B). $C_2H_5OH/H_2O/O_2$ = 1:1.8:0.6 (molar ratio); contact time = 0.6 s g/ml.

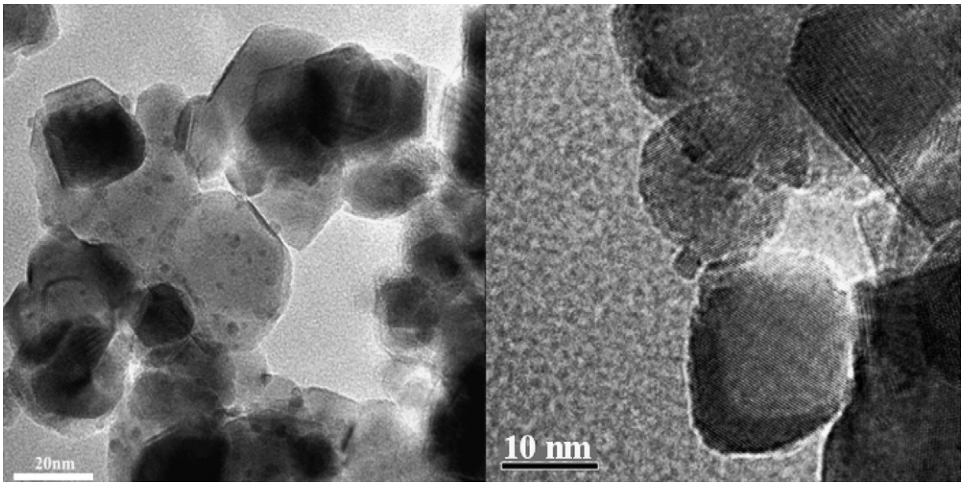

Fig. 6. HRTEM images of the used Rh/CeO_2 for ethanol autothermal reforming at 923 K for 70 h on-stream operation.

concentrations of methane and carbon dioxide decreased significantly. This phenomenon indicated clearly that the steam reforming of methane and the reverse WGS reaction, which were thermodynamically feasible, took place as the major reactions. At 923 K, the outlet stream consisted of 67% H_2, 18% CO, 8% CO_2 and 7% CH_4.

3.3. Stability test

Fig. 5 illustrates the concentrations of H_2, CO_2, CH_4 and CO in the outlet gas of ethanol autothermal reforming over the Rh/CeO_2 for 70 h on-stream at 823 and 923 K. At 823 K, the concentrations of H_2, CO_2, CO and CH_4 were stabilized at 52%, 28%, 8% and 12%, respectively. When the reaction was conducted at 923 K, the concentration of H_2 increased to about 68% closing to thermodynamic equilibrium value, but the concentration of CO_2 decreased rapidly due to the occurrence of the reverse WGS, yielding significantly amounts of CO. As a result, the outlet stream consisted of 68% H_2, 17% CO, 8% CO_2 and 7% CH_4. More importantly, the Rh/CeO_2 catalyst exhibited rather stable activity and selectivity during the 70 h on-stream operation and no obvious deactivation, as expressed by the almost constant effluent compositions, was observed even with a stoichiometric feed composition of ethanol/water/O_2 molar ratio being 1:1.8:0.6, where no excess water and/or oxygen was available to remove carbon deposits that were detrimental to the catalytic stability.

Fig. 1 also presents the XRD patterns of the Rh/CeO_2 catalysts used for ethanol autothermal reforming at 823 and 923 K for 70 h on-stream. There was still no diffraction peak of Rh species, providing further evidence that no aggregation or sintering of Rh particles occurred. However, the particle size of ceria, which was 7 nm in the as-prepared sample, increased significantly to 17 nm at 823 K and 22 nm at 923 K. Nevertheless, it appeared that the growth of ceria particles had no remarkable influence on the performance of the Rh/CeO_2 catalyst. Wang et al. [18] reported previously that CeO_2 particle size in the range of 7–40 nm had almost no effect on the rate of WGS reaction over a Pd/CeO_2 catalyst. It has been suggested that the deactivation of ceria is only associated with the removal of defects in a narrow temperature range, but there is little loss of defects after ceria was heated below 1033 K [19].

Fig. 6 shows the HRTEM images of the Rh/CeO_2 catalyst used for ethanol autothermal reforming at 923 K up to 70 h on-stream. Apparently, the particle size of ceria increased to about 20 nm during the course of reaction. The small ceria nanoparticles with high surface energy in the fresh catalyst tended to aggregate into larger particles under the reaction conditions, similar to a hydrothermal process. However, the Rh particles with size of 1–3 nm were still highly dispersed on the surface of ceria, maintaining sufficient Rh–ceria interfacial areas where the reaction takes place. It seems that ceria particles with sizes in the range of 7–20 nm provide sufficient Rh–CeO_2 interfacial perimeter, i.e. facile activation of water and/or oxygen for a continuous cleaning of carbonaceous entities on the surface of Rh particles, promoting carbon removal. This decoking activity would likely be enhanced through the participation of lattice oxygen, which subsequently would be supplemented with the oxygen from the feed. Therefore, it is highly possible that a dynamic equilibrium between the coke formation and its gasification on the Rh/CeO_2 catalyst has been established during the course of reaction.

4. Conclusions

The Rh/CeO_2 catalyst was highly active and stable for autothermal reforming of ethanol with a stoichiometric feed composition. Ethanol and the reaction intermediates were totally converted to hydrogen and C1 products at 673 K, and methane steam reforming and reverse water gas shift were the major reactions above 823 K. There was no detectable deactivation for 70 h on-stream at 923 K because the ceria support prevented the highly dispersed Rh particles with sizes of 1–3 nm from sintering under the reaction conditions, which maintained sufficient Rh–CeO_2 interfacial areas where the reaction takes place.

Acknowledgement

We gratefully acknowledge the financial support from the National Natural Science Foundation of China (grant number 20773119).

References

[1] M. Ni, D.Y.C. Leung, M.K.H. Leung, Int. J. Hydrogen Energy 32 (2007) 3238.
[2] A.N. Fatsikostas, X.E. Verykios, J. Catal. 225 (2004) 439.
[3] B. Zhang, X. Tang, Y. Li, W. Cai, Y. Xu, W. Shen, Catal. Commun. 7 (2006) 367.
[4] H. Fajardo, L. Probst, Appl. Catal. A 306 (2006) 134.
[5] N. Laosiripojana, S. Assabumrungrat, Appl. Catal. B 66 (2006) 29.
[6] K. Liguras, D.I. Kondarides, X.E. Verykios, Appl. Catal. B 43 (2003) 345.
[7] A. Erdohelyi, J. Rasko, Catal. Today 116 (2006) 367.
[8] S. Cavallaro, V. Chiodo, A. Vita, S. Freni, J. Power Sources 94 (2001) 14.
[9] W. Cai, B. Zhang, Y. Li, Y. Xu, W. Shen, Catal. Commun. 8 (2007) 1588.
[10] G.A. Deluga, J.R. Salge, L.D. Schmidt, X.E. Veryios, Science 303 (2004) 993.

[11] J. Kugai, V. Subramani, C. Song, M.H. Engelhard, Y.H. Chin, J. Catal. 238 (2006) 430.

[12] B.D. Cullity, Elements of X-ray Diffractions, 2nd ed., Addison-Wesley, Menlo Park, CA, 1978, p. 102.

[13] A. Trovarelli, Catal. Rev. Sci. Eng. 38 (1996) 439.

[14] E.M. Sadovskaya, Y.A. Ivanova, L.G. Pinaeva, G. Grasso, T.G. Kuznetsova, A. van Veen, V.A. Sadykov, C. Mirodatos, J. Phys. Chem. A 111 (2007) 4498.

[15] A. Martínez-Arias, J. Soria, J.C. Conesa, J. Catal. 168 (1997) 364.

[16] P.Y. Sheng, W.W. Chiu, A. Yee, S.J. Morrison, H. Idriss, Catal. Today 129 (2007) 313.

[17] P.Y. Sheng, A. Yee, G.A. Bowmaker, H. Idriss, J. Catal. 208 (2002) 393.

[18] X. Wang, R.J. Gorte, J.P. Wagner, J. Catal. 212 (2002) 225.

[19] E. Mamontov, T. Egami, J. Phys. Chem. B 104 (2000) 11110.